Raman spectroscopy for quantification of residual calcium and total ash in mechanically deboned chicken meat

Sileshi Gizachew Wubshet[a]*, Jens Petter Wold[a], Ulrike Böcker[a], Karen Wahlstrøm Sanden[a], Nils Kristian Afseth[a].

[a]Nofima AS - Norwegian Institute of Food, Fisheries and Aquaculture Research, PB 210, N-1431 Ås, Norway

*Corresponding author. Tel.: +47 909 17 126

E-mail address: sileshi.wubshet@nofima.no (Sileshi G. Wubshet).

Key words: Raman spectroscopy, multivariate calibration, mechanically deboned chicken meat, ash, calcium

Abstract

According to European food safety authorities, one of the major control parameters for mechanically separated meat is calcium content, which is an indicator of residual bone. Residual bone in mechanically separated meat can also be measured as a total ash content. Despite the need to measure both ash and/or calcium content of mechanically separated meat, there is no rapid analytical technique that can be used in an industrial environment. In the current study, we are presenting the first application of Raman spectroscopy as a rapid tool for estimating calcium and ash contents in bone and meat mixtures from mechanical deboning of chicken meat. Raman-based partial least squares regression models were developed for prediction of both ash and calcium content in 79 samples gathered from four different production days. Two different data pre-processing methods, i.e., polynomial background fitting and extended multiplicative scattering correction with polynomial extension, were applied to the raw Raman data and the prediction models were compared. The prediction model based on EMSC treated data afforded the lowest root mean square error of cross-validation (RMSECV = 0.333 g/100 g for calcium and RMSECV = 0.634 g/100 g for ash) and the highest coefficient of determination (R^2 = 0.775 for calcium and R^2 = 0.894 for ash).

1. Introduction

Mechanical deboning is an industrial processing technology used for optimal recovery of protein rich meat mince from animal carcasses (Field, 1981; Froning, 1981). This process involves mechanical grinding of the carcasses to form a meat and bone slurry, followed by passing the mixture through a fine screen or slotted surface to separate the meat from the bone-rich residue (Froning, 1981). Mechanical deboning is vastly practiced in the poultry processing industry for separating edible mince from carcasses that have already been through a standard filleting process. Mechanically deboned chicken meat (MDCM) is being used in several food products, e. g., sausages, to increase nutritional and sensory attributes (Mielnik, Aaby, Rolfsen, Ellekjær, & Nilsson, 2002; Song et al., 2014). In addition, both MDCM and the bone rich residual of the separation process, i.e., mechanical deboning residue (MDR), have been used as raw materials for enzymatic protein hydrolysis (Fonkwe & Singh, 1996; Sun, Zhao, Cui, Zhao, & Yang, 2010). Enzymatic hydrolysis of MDCM and MDR have been shown to provide high quality protein hydrolysates that can be used in food and feed formulation (Rossi, Flôres, Heck, & Ayub, 2009). Residual bone content, typically measured as percentage ash or percentage calcium, is a regulated parameter related to quality of mechanically separated meat (EFSA, 2013). Ash content of MDR and MDCM has also been shown to be a crucial factor for the protein yield of an enzymatic hydrolysis process based on these raw materials (Wubshet et al., 2018).

Depending on the process settings and carcass composition, fine granules of bone could be introduced to mechanically separated meat (MSM). Therefore, bone content of MSM is usually controlled by setting calcium or ash limits (Field, 2000). According to the European food safety authority (EFSA), determination of bone (or calcium) content in MSM can also be used to control the yield of the mechanical separation process (EFSA, 2013). Moreover, EFSA

identified calcium content as the only appropriate chemical parameter which can be used to distinguish MSM from non-MSM products (EFSA, 2013).

The currently practiced analytical procedures for determination of calcium in mechanically separated meat are based on atomic absorption spectrophotometry, inductively coupled plasma-optic emission spectrometry and standard titration (Germs & Steunenberg, 1978; Grunden & Macneil, 1973; Tasić et al., 2017). Determination of ash content in such matrices is performed based on a gravimetric measurement after complete ignition of the organic matters. All of the above methods are time consuming and are typically performed offline on analytical scale samples (in the order of few grams). Therefore, the existing methods cannot be directly used to control calcium and ash content in a large scale industrial production. Industrial deboning processes in EU member states are typically performed by setting the separation pressures below 100 bar for the production of low pressure MSM and up to 400 bar for production of high pressure MSM (EFSA, 2013). However, without a process control tool, such arbitrary settings of the separation force cannot always guarantee neither a permissible level of calcium nor an optimal yield. Therefore, an analytical tool that allows the rapid measurement of calcium or ash levels in meat and bone mixtures is vital for quality control and yield optimization.

One of the advanced and attractive technologies for detection and characterization of bone in complex mixtures is Raman spectroscopy. Raman spectroscopy has been extensively used in medical research as a diagnostic tool for qualitative characterization of bone (Mandair & Morris, 2015; Morris & Mandair, 2011). This technique has been shown to provide an excellent insight into both the bone minerals as well as the bone matrix. The sensitivity of Raman spectroscopy for bone minerals, containing carbonated hydroxyapatite as a primary constituent, is due to the vibrational shifts of the phosphate and carbonate groups. The intensity of these two bands is correlated to calcium, a metal that constitutes 60% of total minerals in bone and mainly exists as $Ca_5(PO_4)_3(OH)$. Despite this apparent sensitivity, Raman spectroscopy, has not been

used to quantitatively predict parameters related to bone content, i.e., ash and calcium. In the current study we have developed a partial least squares regression (PLSR) model for prediction of both calcium and ash in bone and meat mixtures from mechanical deboning of chicken meat.

2. Materials and Methods

2.1.Sample materials

All sample materials used in the current study were collected from a Norwegian poultry processing plant (Nortura, Hærland, Norway). MDCM and MDR of freshly slaughtered fowls were collected on four different days. The force of mechanical separation on all the four days was set to yield 50 % (v/v) meat fraction from a given raw material. In order to obtain relevant variation of bone content, a series of MDCM and MDR mixtures were prepared by varying the ratios of the two. A total of 79 samples were prepared from the four different production dates.

2.2.Reference measurements (percentage calcium, ash and bone)

All sample materials were homogenized using a food processor prior to reference measurement. Calcium measurements were performed according to NS-EN ISO 17294-2 (ISO, 2016). In short, approximately 1 g of sample was weighed and incinerated in a muffle furnace at 550°C. The ash was then mixed with HCl and boiled. The mixture was filtered and diluted prior to analysis by inductively coupled plasma mass spectrometry (ICP-MS). The ash measurements were performed according to the NMKL 173 2nd edition (2005) with slight modification (NMKL, 2005). Approximately 5 g of sample was weighed in a porcelain dish and placed in a muffle furnace at room temperature. The furnace was turned on and the samples were incinerated for 16-18 hours at 550^0C ± 25^0C and then cooled in a desiccator before they were weighed.

2.3.Raman spectroscopy

For the Raman measurements, approximately 500 g of each sample were arranged in aluminum box with dimensions 3 cm × 16 cm × 20 cm (height × length × width). The measurements were carried out using a RamanRXN2^{TM} Hybrid system equipped with a non-contact PhAT-probe (Kaiser Optical Systems, Inc., Ann Arbor, MI). The excitation wavelength was 785 nm with a spot size of 6 mm at 25 cm working distance. Raman spectra were collected in a range from

175 to 1875 cm^{-1} with an accumulation time of 15 sec × 4. The samples were moved manually in a zigzag pattern under the laser beam to secure representative sampling (Wubshet et al., 2018). Samples from production day 1 and day 2 were measured on the same day, whereas samples from production day 3 and 4 were measured a week later.

2.4.Pre-processing

Two different preprocessing methods, i.e., polynomial background correction and extended multiplicative signal correction (EMSC) with polynomial extension (Afseth & Kohler, 2012; Liland, Kohler, & Afseth, 2016) , were used. The EMSC model used in this study was based on the methodology described in the tutorial by Afseth and Kohler (Afseth & Kohler, 2012). In short, the spectra were trimmed into a range 650 cm^{-1} to 1775 cm^{-1} and the EMSC corrected spectra were calculated using the following formula:

$$A_{corr}(\tilde{v}) = \frac{A(\tilde{v}) - a - d_1\tilde{v} - d_2\tilde{v}^2 - \cdots - d_n\tilde{v}^n}{b}$$

where $A_{corr}(\tilde{v})$ is the EMSC corrected version of the Raman scattering intensity at wavenumber *v* and $A(\tilde{v})$ is the Raman scattering intensity at wavenumber *v*. $\tilde{v}^j$ are polynomials of wavenumbers *v* with the corresponding constants d_j. *a* and *b* are, respectively, the offset and a multiplicative constant. The mean spectrum of all the 79 spectra was subjected to polynomial baseline correction (forth order) and used as a reference in the EMSC correction.

For the polynomial background correction, an automated method originally developed by Lieber & Mahadevan-Jansen was used (Lieber & Mahadevan-Jansen, 2003). Similar to the EMSC procedure the spectra were trimmed into a range from 650 cm^{-1} to 1775 cm^{-1}. The trimmed spectra were then subjected to an iterative procedure where the baseline of each spectrum was estimated through successive polynomial fittings. The maximum number of iteration was set to 1000 and the repetition was stopped when the difference between the baseline and the fitted polynomial is sufficiently small (as decided by a convergence criterion).

For this procedure a polynomial degree of 4 was used. Finally, the fitted baseline was subtracted from the raw spectrum to afford the baseline corrected spectrum. In addition, to the corrected spectra the fitted polynomial baseline was also extracted from every spectrum and used in the statistical analysis. Both the EMSC correction the polynomial background correction were performed using in-house scripts automated from MATLAB software (R2013b, The MathWorks, Inc., Natick, MA, USA).

2.5.Statistical analysis

In order to study the overall variation in the dataset, principal component analysis (PCA) was performed on the EMSC corrected Raman spectra. The spectral range used for the PCA was from 650 cm^{-1} to 1775 cm^{-1}. A full cross-validation of the PCA was performed by leaving one of the spectra out at a time. A multivariate regression model, using PLSR, was developed to predict the content of calcium and ash using Raman spectra of 79 samples from a mechanical chicken deboning process. The optimal number of PLSR factors was determined by the contiguous-block-out cross-validation method, where a block samples from one of the four sampling days were held out at a time. The developed prediction models were evaluated using root mean square error of cross-validation (RMSECV) and the coefficient of determination (R^2) between the reference and predicted values. Four regression models were developed using the raw spectra, the EMSC-corrected spectra, the spectra after polynomial background correction and the fluorescence background extracted using the polynomial background correction algorithm, respectively. Both PCA and PLSR were performed using The Unscrambler® X v10.3 (CAMO Software AS, Oslo, Norway).

3. Results and Discussion

3.1. Ash and calcium content

Ash and calcium content of a total of 79 samples, obtained from mechanical separation of chicken meat, were studied using Raman spectroscopy and multivariate statistics. By evaluating the reference measurements, a positive correlation ($R^2 = 0.757$) was observed between calcium and ash content of the samples (Figure 1). This was expected as the calcium to ash ratio in broilers is constant at approximately 37% (Norris, Kratzer, Lin, Hellewell, & Beljan, 1972). However, a small variation may occur due to anatomical structure of different breeds and feeding regimens (Field, 2000). For broilers the amount of fresh bone can be calculated from percentage calcium using a conversion factor of 5 (Field, 2000). Hence, both ash and calcium content have been used as a measure of bone content in matrices such as mechanically deboned meat (Field, 2000).

3.2.Raman spectral profiling

Raw, polynomial baseline corrected and EMSC corrected spectra and the extracted polynomial baseline of all the 79 samples are presented in Figure 2. The spectra, colored according to the % calcium levels of each sample, showed two important trends. The first one was an increase in fluorescence background for each sample with an increase in % calcium level (Figure 2A, 2C). This was apparent from the fluorescent bone matrices as well as the connective tissues associated with residuals of the mechanical deboning. Fluorescence background is a well-known challenge in Raman studies of bone tissue and, in some cases, requires special acquisition procedures such as photo-bleaching to avoid this competing phenomenon (Golcuk et al., 2006). In the present study, in order to subtract the background associated with fluorescence, two different pre-processing methods (i. e., a standard polynomial fit and EMSC with polynomial extension) were used. In addition to the fluorescence-associated baseline

correction the EMSC approach also involves a normalization step to remove multiplicative effects due to, for example, difference in laser focusing.

The second important systematic trend correlating with the % calcium level was the intensity of the phosphate band ($\nu_1PO_4^{3-}$) at 960 cm^{-1}. This correlation was apparent, since calcium is a major bone mineral and exists mainly as a phosphate salt (i.e., hydroxyapatite, $Ca_5(PO_4)_3(OH)$). While $\nu_1PO_4^{3-}$ is the widely used mineral band, the carbonate band at 1070, cm^{-1}($\nu_1CO_3^{2-}$) and a component of a phosphate band at 1076 cm^{-1}($\nu_3PO_4^{3-}$) are also characteristic fingerprints of bone mineral (Mandair & Morris, 2015). In this study, these bands were observed highly overlapping with the ν(C-O) and ν(C-C). In addition to the mineral bands, EMSC corrected Raman spectra of all samples showed predominant bands origination mainly from the fat component of the raw materials. Previous studies have shown that fat content of MDM and MDR can be as high as 27.3 and 16.9 percent, respectively (Wubshet et al., 2018). The less pronounced bands from the protein, such as amide I and III, are overlapping with the vibrational shifts of the fatty acids. Tentative assignments of the major bands presented in Figure 2D was based on previous Raman studies on chicken meat and bone minerals (Mo, Zheng, & Huang, 2010).

3.3.Principal component analysis

In order to study the most important spectral variations, potential outliers and systematic artifacts in the sample set, PCA was performed on the EMSC corrected Raman spectra. The first three principal components (PCs) explained 89% of the total variation in the data set. The first principal component (PC-1), explaining 72% of the variation, is related to the bone content of the sample. This was deduced from the strong correlation of the score values in PC-1 against percentage ash and calcium values of individual samples (Figure 3C and 3D). The loading plot of PC-1 revealed that the phosphate band ($\nu_1PO_4^{3-}$) at approximately 960 cm^{-1} was the most important variable for the observed variation in this PC (Figure 4A).

The second and third principal component (PC-2 and PC-3), collectively explaining 17% of the total variation, highlights differences between the samples collected on the four different production days. The major bands observed in loading plot for PC-2 were C-C stretching (1062 cm^{-1} and 1129 cm^{-1}), C-C bending and twisting (1296 cm^{-1}) and C=C stretching (1659 cm^{-1}). These bands have previously been associated with fat content and degree of unsaturation of fatty acids (Lee et al., 2018). Hence, the observed classification along PC-2 could be due to variations in fat composition of the different broiler flocks processed on the different sampling days. Factors such as different feeding regimens have previously been reported to result in differences in fatty acid composition of different flocks of fowls (Khaled, John, Robert, Beverly, & Robert, 2018). The classification observed in PC-3 was consistent with the two different measurement days. Raman measurements of samples from day 1 and 2 were performed on a different day than samples from day 3 and 4. The observed clear distinction between the two measurement days is most likely due to different experimental conditions, e.g., the atmospheric and optical variation, as proven by the sharp peaks in the loading plot (Figure 4C).

3.4.Partial least square regression

PLSR models were developed for prediction of ash and calcium content of the samples using the raw spectra, the polynomial baseline corrected spectra, the EMSC corrected spectra, and the extracted polynomial baseline. The number of latent components, coefficients of determination (R^2) and root mean square error of predictions (RMSECV) are given in Table 1. Of the four data sets, the EMSC corrected set afforded a prediction model with a higher correlation coefficient (R^2 = 0.894 for calcium and R^2 = 0.775 for ash) and lower prediction error (RMSECV = 0.634 for calcium and RMSECV = 0.333 for ash). This is consistent with previous studies, which have shown improved prediction models with EMSC corrected Raman spectra compared to other conventional pre-processing methods (Liland et al., 2016). The polynomial

baseline corrected spectra also gave an improved model compared to the raw Raman spectra for prediction of both % ash (R^2 = 0.863; RMSECV = 0.779) and % calcium (R^2 = 0.759; RMSECV = 0.348). The similarity between prediction models obtained from EMSC-corrected and baseline-corrected spectra, respectively, indicate that the normalization procedure included in the former preprocessing step is not crucial for the model. This is most likely related to the fact that the Raman probe used in the study, i.e. the non-contact PhAT-probe, provides a large laser spot-size and high focal volume. This means that there are less spectrum-to-spectrum intensity variations related to focusing differences, and thus less need for a standard normalization approach.

One of the interesting observations was the performance of the model based on the extracted polynomial baselines. Despite appearing as a general baseline offset, the extracted fluorescence baseline showed a reasonable correlation with both % ash (R^2 = 0.851) and % calcium (R^2 = 0.732). The PLSR model based on this data set was also comparable with the one obtained from the raw Raman data. This was interpreted to be a result of the correlation between fluorescent fresh bone matrices and the bone minerals (i.e., measured as ash and calcium in this study). Therefore, the observed prediction performance for bone minerals are based on this indirect correlation with the fluorescent bone matrices. However, since other components, such as connective tissues can contribute to variation in the fluorescence background, the application of such model based approach on an indirect correlation can be highly uncertain. The regression coefficients of all the models based on EMSC and polynomial baseline corrected Raman spectra are presented in Figure 5. As expected, the phosphate band at 960 cm^{-1} was observed as the major variable for the models based on the polynomial baseline corrected and EMSC corrected datasets.

Overall, we have demonstrated the potential of Raman spectroscopy as a rapid tool for estimation of ash and calcium in meat and bone mixtures from mechanical deboning of chicken

meat. In contrast to the existing methods for measuring calcium content, e.g. titration, the present strategy is rapid and requires minimal or no sample pre-treatments. The titration based method presented by Tasić *et al.* (2017) for determination of calcium content in mechanically separated meat requires digestion of sample materials in a solution of hydrochloric acid prior to the titrimetric determinations (Tasić et al., 2017). Another significant advantage of the presented method is the ability to obtain representative sampling. The amount of sample used for analysis of calcium based on methods such as, atomic absorption spectrometry, is typically 10 mg or less (Grunden & Macneil, 1973). This poses a significant challenge as measurements on such a small amount of sample from inhomogeneous mixtures of bone and mince can be uncertain due to lack of representative sampling. In contrast to this, the Raman setup presented here can probe a larger volume of a sample by contentiously illuminating and acquiring data while moving the sample under a fixed probe. This is a very important advantage, especially, when considering the volume of production from an industrial mechanical deboning process.

4. Conclusions

The present work reports application of Raman spectroscopy for estimation of calcium and ash content in bone and meat mixtures from mechanical deboning of chicken. Multivariate calibration models were developed for prediction of ash and calcium contents in samples gathered from a Norwegian poultry processing plant. Two preprocessing strategies, i.e. polynomial background correction and EMSC with polynomial extension, were evaluated before developing Raman-based PLSR models for prediction of % ash and % calcium. EMSC correction was shown to yield a model with highest R^2 and lowest prediction error. To the authors' knowledge, the presented work is the first application of Raman spectroscopy for quantitative estimation of bone minerals in complex mixtures from mechanical deboning of meat. Therefore, this technique holds a promising potential as industrially feasible on- or at-line tool for controlling quality of mechanically deboned chicken meat or similar food matrices.

Further work in expanding the calibration data set as well as optimizing the data acquisition setup are required in order to develop a robust prediction models that can be used in an industrial process control.

Acknowledgments

Financial support from the Norwegian Research Council through the project iProcess (255596/E50) and the Norwegian Agricultural Food Research Foundation through the project FoodSMaCK — Spectroscopy, Modelling and Consumer Knowledge (262308/F40), is greatly acknowledged. Nortura, Hærland, Norway is acknowledged for providing raw materials used in this study.

341 **References**

342 Afseth, N. K., & Kohler, A. (2012). Extended multiplicative signal correction in vibrational
343 spectroscopy, a tutorial. *Chemometrics and Intelligent Laboratory Systems, 117*, 92-
344 99.

345 EFSA (European Food Safety Authority) (2013). Scientific opinion on the public health risks
346 related to mechanically separated meat (MSM) derived from poultry and swine. *EFSA*
347 *Journal, 11*(3):3137, pp 1-78

348 Field, R. A. (1981). Mechanically Deboned Red Meat. In C. O. Chichester, E. M. Mrak, & G.
349 F. Stewart (Eds.), *Advances in Food Research* (Vol. 27, pp. 23-107): Academic Press.

350 Field, R. A. (2000). Ash and calcium as measures of bone in meat and bone mixtures. *Meat*
351 *Science, 55*(3), 255-264.

352 Fonkwe, L. G., & Singh, R. K. (1996). Protein recovery from mechanically deboned turkey
353 residue by enzymic hydrolysis. *Process Biochemistry, 31*(6), 605-616.

354 Froning, G. W. (1981). Mechanical deboning of poultry and fish. In C. O. Chichester, E. M.
355 Mrak, & G. F. Stewart (Eds.), *Advances in Food Research* (Vol. 27, pp. 109-147):
356 Academic Press.

357 Germs, A. C., & Steunenberg, H. (1978). Estimating calcium in mechanically deboned
358 poultry meat by oxidimetry and atomic absorption spectrophotometry. *Food*
359 *Chemistry, 3*(3), 213-219.

360 Golcuk, K., Mandair, G. S., Callender, A. F., Sahar, N., Kohn, D. H., & Morris, M. D. (2006).
361 Is photobleaching necessary for Raman imaging of bone tissue using a green laser?
362 *Biochimica et Biophysica Acta (BBA) - Biomembranes, 1758*(7), 868-873.

Grunden, L. P., & Macneil, J. H. (1973). Examination of bone content in mechanically deboned poultry meat by EDTA and atomic absorption spectrophotometric methods. *Journal of Food Science, 38*(4), 712-713.

ISO 17294-2 Application of inductively coupled plasma mass spectrometry (ICP-MS) - Part 2: Determination of selected elements including uranium isotopes. (2016)

Khaled, K., John, C., Robert, H., Beverly, M., & Robert, G. (2018). The effect of different dietary fats on the fatty acid composition of several tissues in broiler chickens. *European Journal of Lipid Science and Technology, 120*(1), 1700237(1-33).

Lee, J.-Y., Park, J.-H., Mun, H., Shim, W.-B., Lim, S.-H., & Kim, M.-G. (2018). Quantitative analysis of lard in animal fat mixture using visible Raman spectroscopy. *Food Chemistry, 254*, 109-114.

Lieber, C. A., & Mahadevan-Jansen, A. (2003). Automated method for subtraction of fluorescence from biological Raman spectra. *Applied Spectroscopy, 57*(11), 1363-1367.

Liland, K. H., Kohler, A., & Afseth, N. K. (2016). Model-based pre-processing in Raman spectroscopy of biological samples. *Journal of Raman Spectroscopy, 47*(6), 643-650.

Mandair, G. S., & Morris, M. D. (2015). Contributions of Raman spectroscopy to the understanding of bone strength. *BoneKEy Reports, 4*, 620(1-8).

Mielnik, M. B., Aaby, K., Rolfsen, K., Ellekjær, M. R., & Nilsson, A. (2002). Quality of comminuted sausages formulated from mechanically deboned poultry meat. *Meat Science, 61*(1), 73-84.

Mo, J., Zheng, W., & Huang, Z. (2010). Fiber-optic Raman probe couples ball lens for depth-selected Raman measurements of epithelial tissue. *Biomedical Optics Express, 1*(1), 17-30.

Morris, M. D., & Mandair, G. S. (2011). Raman assessment of bone quality. *Clinical Orthopaedics and Related Research®, 469*(8), 2160-2169.

Nordic Committee on Food Analysis (NMKL). Ash, gravimetric determination in foods. Method no. 173, 2nd Ed (2005).

Norris, L. C., Kratzer, F. H., Lin, H. J., Hellewell, A. B., & Beljan, J. R. (1972). Effect of quantity of dietary calcium on maintenance of bone integrity in mature white leghorn male chickens. *The Journal of Nutrition, 102*(8), 1085-1091.

Rossi, D. M., Flôres, S. H., Heck, J. X., & Ayub, M. A. Z. (2009). Production of high-protein hydrolysate from poultry industry residue and their molecular profiles. *Food Biotechnology, 23*(3), 229-242.

Song, D.-H., Choi, J.-H., Choi, Y.-S., Kim, H.-W., Hwang, K.-E., Kim, Y.-J., Ham, Y. –K., & Kim, C.-J. (2014). Effects of mechanically deboned chicken meat (MDCM) and collagen on the quality characteristics of semi-dried chicken jerky. *Korean Journal for Food Science of Animal Resources, 34*(6), 727-735.

Sun, W., Zhao, M., Cui, C., Zhao, Q., & Yang, B. (2010). Effect of Maillard reaction products derived from the hydrolysate of mechanically deboned chicken residue on the antioxidant, textural and sensory properties of Cantonese sausages. *Meat Science, 86*(2), 276-282.

405 Tasić, A., Kureljušić, J., Nešić, K., Roković, N., Vićentijević, M., Radović, M., & Pisinov, B.
406 (2017). Determination of calcium content in mechanically separated meat. *IOP*
407 *Conference Series: Earth and Environmental Science, 85*(1), 012056 (1-5).

408 Wubshet, S. G., Wold, J. P., Afseth, N. K., Böcker, U., Lindberg, D., Ihunegbo, F. C., &
409 Måge, I. (2018). Feed-forward process control in enzymatic protein hydrolysis of
410 poultry by-products: A spectroscopic approach. *Food and bioprocess technology,* In
411 press https://doi.org/10.1007/s11947-018-2161-y.

412

413

414

415

416

417

418

419

420

421

422

423

424

425 **Table captions**

426 Table 1. PLR results for prediction of % ash and % calcium from Raman spectra. The presented
427 four different models were developed based on the raw spectra, polynomial baseline corrected
428 spectra, EMSC corrected spectra and the extracted polynomial baseline.

429

430

431

432

433

434

435

436

437

438

439

440

441

442

443

444

445 **Figure captions**

446 Figure 1. Correlation of % ash and % calcium values for 79 samples from mechanical deboning
447 of chicken.

448 Figure 2. Raw (A), polynomial baseline corrected (B) and EMSC-corrected (D) Raman spectra
449 of the 79 samples from mechanical deboning of chicken. The baseline extracted during the
450 polynomial baseline correction are presented in sub-figure C. All spectra are color-weighed
451 according the % calcium. Assignment of the major bands are shown in sub-figure D.

452 Figure 3. Score plots (PC-1 vs PC-2 (A) and PC-2 vs PC-3 (B)) from principal component
453 analysis of the EMSC-corrected Raman data obtained for the 79 samples from mechanical
454 deboning of chicken. Correlation of score values in PC-1 with % calcium and % ash values is
455 presented in sub-plot C and D, respectively.

456 Figure 4. Loading plots (PC-1 (A), PC-2 (B) and PC-3 (C)) from principal component analysis
457 of the EMSC corrected Raman data obtained for the 79 samples from mechanical deboning of
458 chicken.

459 Figure 5. Regression coefficient plots of the PLSR models based on EMSC corrected (A) and
460 polynomial base line corrected (B) Raman data of 79 samples from mechanical deboning of
461 chicken.

462

463

464

465

466

Tables

Table 1.

Data set	PLSR model for % ash			PLSR model for % calcium		
	No. of components	Coefficient of determination (R^2)	RMSECV in g/100 g	No. of components	Coefficient of determination (R^2)	RMSECV in g/100 g
Raw data	3	0.872	0.806	3	0.734	0.459
Polynomial baseline corrected data	2	0.863	0.779	3	0.759	0.348
EMSC corrected data	2	0.894	0.634	3	0.775	0.333
Extracted polynomial baseline	4	0.851	1.065	4	0.732	0.577

Figures

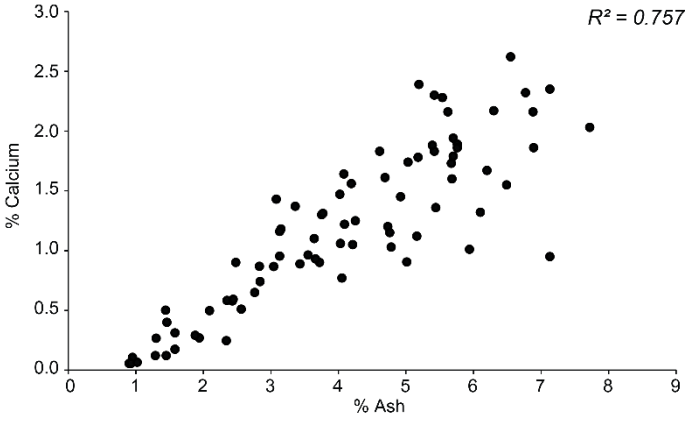

Figure 1

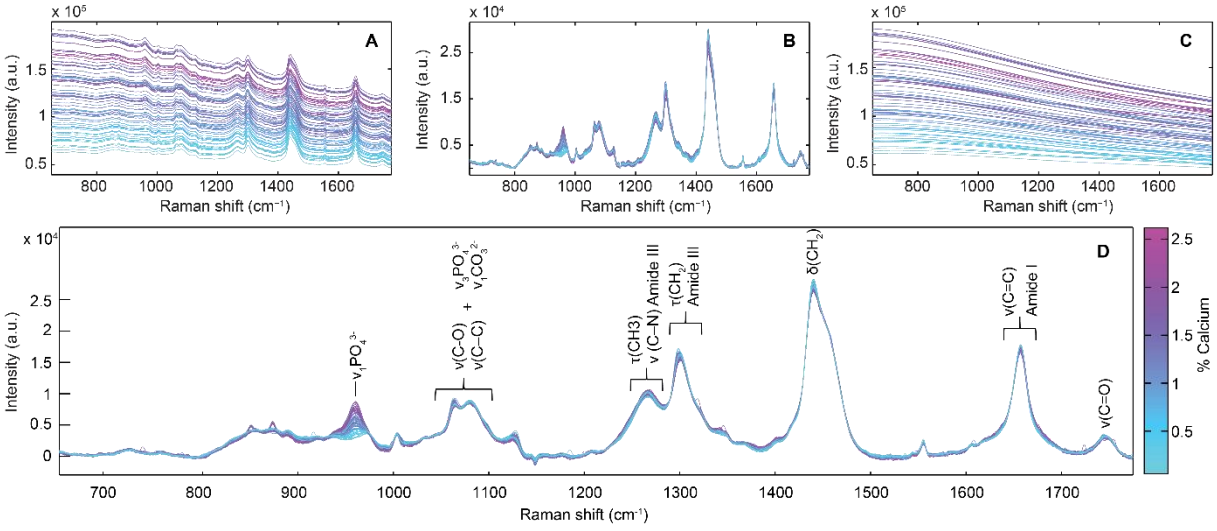

Figure 2.

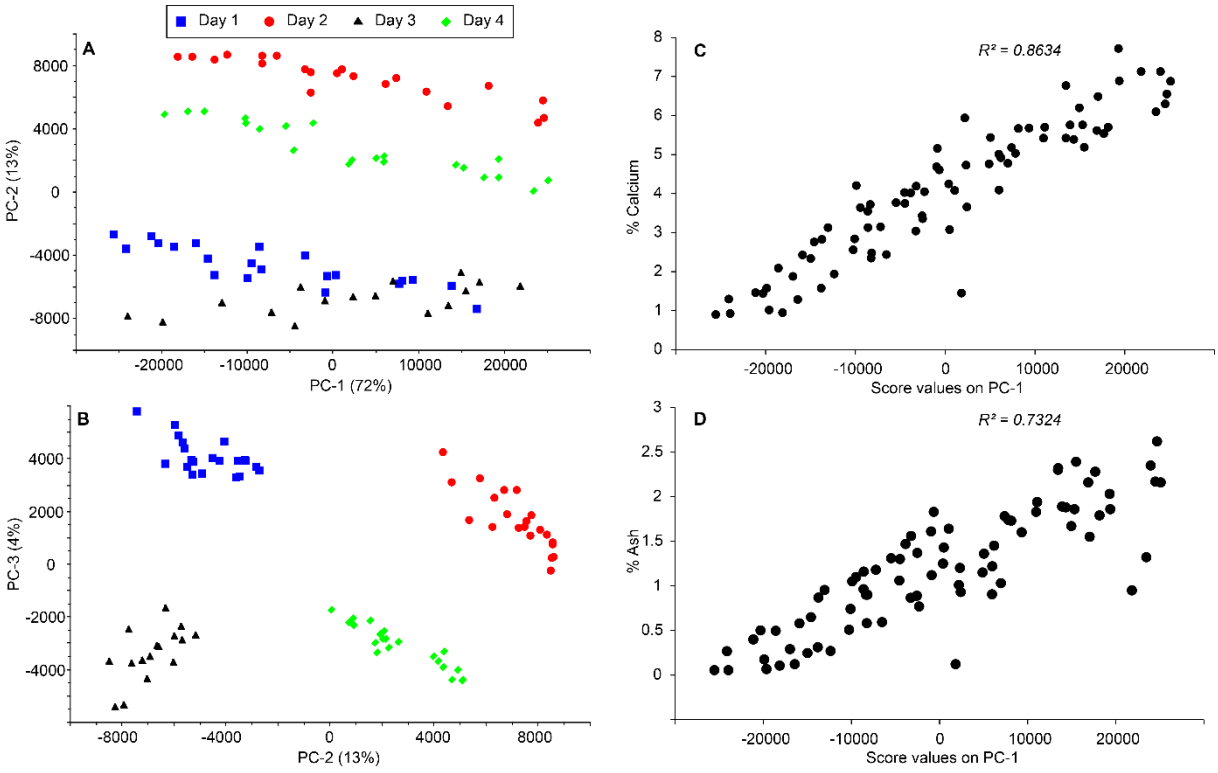

493

494 Figure 3.

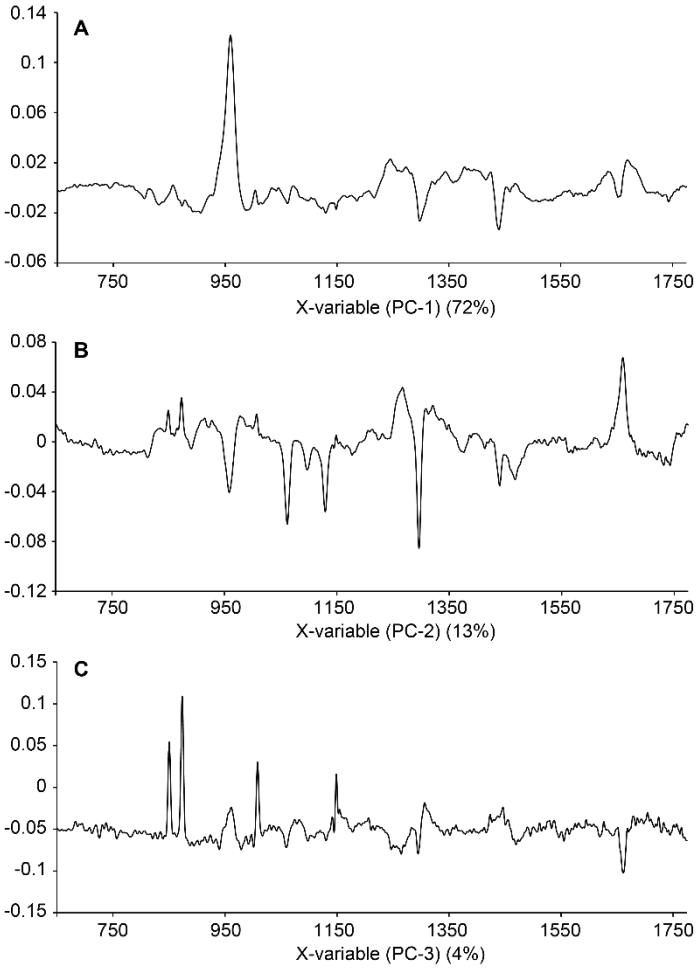
A
0.14
0.1
0.06
0.02
-0.02
-0.06
750
950
1150
1350
1550
1750
X-variable (PC-1) (72%)
B
0.08
0.04
0
-0.04
-0.08
-0.12
750
950
1150
1350
1550
1750
X-variable (PC-2) (13%)
C
0.15
0.1
0.05
0
-0.05
-0.1
-0.15
750
950
1150
1350
1550
1750
X-variable (PC-3) (4%)

Figure 4.

505

506

507

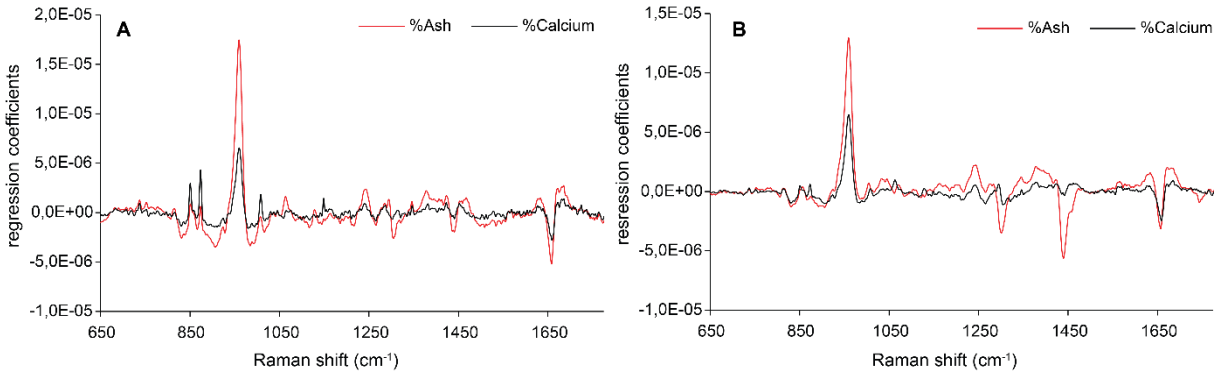

508

509 Figure 5.

510

511

512